A Robust Iris Localization Method Using an Active Contour Model and Hough Transform

Jaehan Koh, Venu Govindaraju, and Vipin Chaudhary
Department of Computer Science and Engineering, University at Buffalo (SUNY)
{jkoh,govind,vipin}@buffalo.edu

Abstract

Iris segmentation is one of the crucial steps in building an iris recognition system since it affects the accuracy of the iris matching significantly. This segmentation should accurately extract the iris region despite the presence of noises such as varying pupil sizes, shadows, specular reflections and highlights. Considering these obstacles, several attempts have been made in robust iris localization and segmentation. In this paper, we propose a robust iris localization method that uses an active contour model and a circular Hough transform. Experimental results on 100 images from CASIA iris image database show that our method achieves 99% accuracy and is about 2.5 times faster than the Daugman's in locating the pupillary and the limbic boundaries.

1. Introduction

Biometrics is the science of automated recognition of persons based on one or multiple physical or behavioral characteristics. Among several biometrics, iris biometrics have gained lots of attention recently because it is known to be one of the best biometrics [4] [15]. Also, iris patterns possess a high degree of randomness and uniqueness even between monozygotic twins and remain constantly stable throughout human's life. Additionally, encoding and matching are known to be reliable and fast [4] [15] [11].

One of the most crucial steps in building an iris security system is iris segmentation in the presence of noises such as varying pupil sizes, shadows, specular reflections and highlights. The step definitely affects the performance of the iris security system since the iris code is generated from the iris pattern and the pattern is affected by iris segmentation. Thus, for a secure iris recognition system, robust iris segmentation is a prerequisite. However, two best known algorithms by Daugman and Wildes [4] [15] along with other algorithms are tested on their private database, making it hard to compare the performance among algorithms. Also, subject cooperation and the good image quality are necessary for both methods to get the maximum performance [15]. Thus, there is a growing need for a robust iris recognition system that requires little subject cooperation and works well under varying conditions. In this paper, we propose a robust iris segmentation algorithm that localizes the pupillary boundary and the limbic boundary based on an active contour model and a circular hough transform. One advantage of our method is that it accurately localizes the pupillary boundary even though the priori estimate is set inaccurately. Experimental results on 100 randomly chosen iris images from one of the widely used public iris image database, CASIA version 3, show that our method outperforms Daugman's approach.

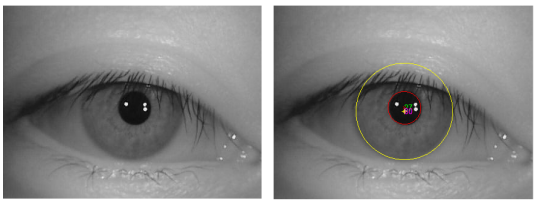

Figure 1. Iris localization

2. Related Work

The iris segmentation involves the following two steps: data acquisition and iris segmentation. The data acquisition step obtains iris images. In this step, infrared illumination is widely used for better image quality. The iris segmentation step localizes an iris region in the image using boundary detection algorithms. Several noises are suppressed or removed in this step. There are many attempts in the area of iris localization and segmentation. The first attempt was made by Daugman *et al.* [4] [5] [6] [7] [8] and Wildes *et al.* [15] [16]. Daugman's method is widely considered as the best iris recognition algorithm. It is reported to achieve a false accept rate (FAR) of one in four million along with a

false reject rate (FRR) of 0. In the image acquisition step, they used several thousand eye images that are not publicly available. In the segmentation step, the iris is modeled as two circular contours and is localized by an integro-differential operator

$$\max_{(r,x_0,y_0)} \left| \frac{\partial}{\partial r} G_\sigma(r) * \oint_{r,x_0,y_0} \frac{I(x,y)}{2\pi r} ds \right|,$$

where $I(x,y)$ represents the image intensity at location (x,y), $G_\sigma(r)$ is a smoothing function with a Gaussian scale σ, and $*$ denotes convolution. The operator searches for the maximum in the blurred partial derivatives in terms of increasing radius r of the normalized contour integral of $I(x,y)$ along a circular arc ds of radius r and center coordinates (x_0,y_0). Also, the eyelids are models as parabolic arcs. The Wildes' system also claims that it achieves a 100% verification accuracy when tested on 600 iris images. As in Daugman's case, the iris images used in Wildes' system are not publicly available. In the segmentation step, they used the gradient-based Hough transform to form two circular boundaries of an iris. The eyelids are modeled as parabolic arcs. Some researchers have tested their iris localization algorithms using the public image database. Ma *et al.* [11] developed algorithms and tested them on CASIA version 1 data set that contains manually edited pupils. They reported a classification rate of 99.43% along with the FAR of 0.001% and the FRR of 1.29%. In the segmentation step, the iris images are projected to the vertical and horizontal directions in order to estimated the center of the pupil. Based on this information, the pupillary boundary (between the pupil and the iris) and the limbic boundary (between the iris and sclera) are extracted. Chin *et al.* [3] reported 100% accuracy on CASIA version 1 data set. In the segmentation step, they employed an edge map generated from a Canny edge detector. Then, a circular Hough transform is used to obtain iris boundaries. Pan *et al.* [13] proposed an iris localization algorithm based on multiresolution analysis and curve fitting. They test their algorithm using CASIA version 2 database, claiming to work better than both the Daugman's algorithm and the Wildes' algorithm in terms of accuracy (*i.e.,* the failure enrollment rate and the equal error rate) and efficiency (*i.e.,* localization time). He *et al.* [9] [10] proposed a localization algorithm using AdaBoost and the mechanics of Hooke's law. They tested the method on CASIA version 3 database, achieving 99.6% accuracy. As we reviewed, most of iris segmentation algorithms are evaluated in terms of detection rate and speed or accuracy and efficiency.

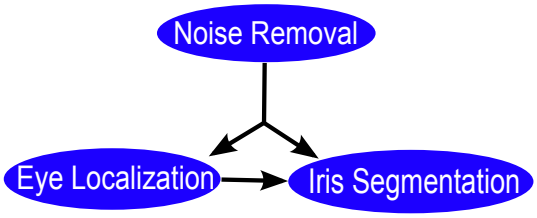

Figure 2. Overview of our method

3. Method

3.1. Problem Definition

In this paper, the iris region is localized and segmented from the image database that is publicly available under the presence of noise. Fig. 1 briefly shows this process. The image on the left is an ROI that cuts off the original image. The one on the right in Fig. 1 contains two circles that represent a pupillary boundary and a limbic boundary along with their respective radii in pixel.

3.2. Overview of Our Method

Our segmentation algorithm broadly consists of the following three stages as in Fig. 2: eye localization, noise removal and iris segmentation. The eye localization estimates the center of the pupil as a circle. The noise removal reduces the effects of noise by Gaussian blurring and morphology-based region filling. The iris segmentation finds the center coordinate of two circles and their associated radii, representing the pupillary boundary and the limbic boundary respectively.

The algorithm runs in the following sequence. Once an ROI having the pupil and the iris of an eye is selected, noises are suppressed by Gaussian blurring. Then the image is binarized, histograms are generated, and the center of the pupil is estimated based on the histograms. Since the estimated center of the pupil in the ROI can be erroneous as in Fig. 4, the iris segmentation based on an active contour model is performed to overcome the false initial estimate. Next the noisy holes in segmentation result are removed by a morphology-based region filling. After that the pupillary boundary is computed by applying the Hough transform to a Canny edge detector. Once the pupillary boundary is localized, it is removed forcibly. The Hough transform is carried out once again for localizing the limbic boundary. Segmentation by the active contour model and the circular Hough transform makes our method robust to initialization errors caused by noises.

3.3. Eye Localization

In this step, an ROI is computed by selecting the eye image that contains the pupil and the iris. An ROI should include as much pupil and iris regions possible while minimally having boundary skin regions. This process reduces the computational burden of future image processing since the size of the image gets smaller without degrading the performance of segmentation. Empirically, two thirds of the center regions of the given image contain the pupil and the iris.

Then the iris image is binarized according to the thresholding method defined as follows:

$$I_{out}(x,y) = \begin{cases} 1 & \text{if } I_{in}(x,y) \geq \tau \\ 0 & \text{otherwise} \end{cases}, \quad (1)$$

where I_{in} is an original image before thresholding and I_{out} is the resulting image after thresholding, Empirically, a threshold τ of 0.2 is used. After binarization, the histograms for both directions are generated by projecting the intensity of the image to the horizontal direction and the vertical direction as in Fig. 3. Then the center coordinate of the pupillary boundary is estimated by the following equations since the pixel intensity of the pupil is lowest across all iris images:

$$\begin{aligned} \overline{x_0} &= \underset{x}{\operatorname{argmin}}\left(\textstyle\sum_y I(x,y)\right), \\ \overline{y_0} &= \underset{y}{\operatorname{argmin}}\left(\textstyle\sum_x I(x,y)\right), \end{aligned} \quad (2)$$

where $\overline{x_0}, \overline{y_0}$ are the estimated center coordinates of the pupil in the original image $I(x,y)$. The estimated center of the pupil is used in the task of pupil localization based on a Chan-Vese active contour model. The Chan-Vese active contour algorithm solves a subcase of the segmentation problem formulated by Mumford and Shah [2].

Specifically, the problem is described as follows: given an image u_0, find a partition Ω_i of Ω and an optimal piecewise smooth approximation u of u_0 such that u smoothly evolves within each Ω_i and across the boundaries of Ω_i. To solve this problem, Mumford and Shah [12] proposed the following minimization problem:

$$\begin{aligned} \inf_C \Big\{ & F^{MS}(u,C) = \textstyle\int_\Omega (u-u_0)^2 dxdy \\ & + \mu \textstyle\int_{\Omega\setminus C} |\nabla u|^2 dxdy + \nu|C| \Big\} \end{aligned}, \quad (3)$$

If the segmented image u is restricted to piecewise constant function inside each connected component Ω_i, then the problem becomes the minimal partitioning problem and its function is given by

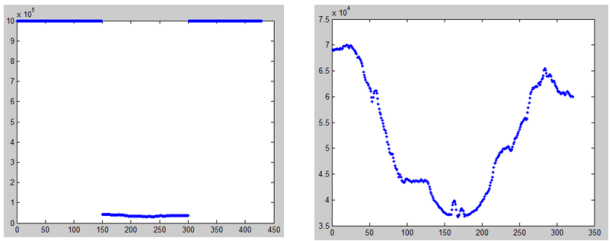

Histogram after projection to the horizontal direction

Histogram after projection to the vertical direction

Figure 3. Histograms of a binarized ROI

$$F^{MS}(u,C) = \sum_i \int_\Omega (u-c_i)^2 dxdy + \nu|C|, \quad (4)$$

According to Chan and Vese [2], given the curve $C = \partial\omega$ where $\omega \in \Omega$, an open subset and two unknown constants c_1 and c_2 as well as $\Omega_1 = \omega$ and $\Omega_2 = \Omega - \omega$, the minimum partitioning problem becomes the problem of minimizing the energy functional with respect to c_1, c_2, and C in accordance with:

$$\begin{aligned} F(c_1,c_2,C) = & \textstyle\int_{\Omega_1=\omega} (u_0(x,y)-c_1)^2 dxdy \\ & + \textstyle\int_{\Omega_2=\Omega-\omega} (u_0(x,y)-c_2)^2 dxdy + \nu|C| \end{aligned}, \quad (5)$$

In level set formulation, C becomes $\{(x,y)|\phi(x,y) = 0\}$. Thus, the energy functional becomes

$$\begin{aligned} F(c_1,c_2,C) = & \textstyle\int_\Omega (u_0(x,y)-c_1)^2 H(\phi) dxdy \\ & + \textstyle\int_\Omega (u_0(x,y)-c_2)^2 (1-H(\phi)) dxdy \\ & + \nu \textstyle\int_\Omega |\nabla H(\phi)| \end{aligned}, \quad (6)$$

where $H(\cdot)$ is a Heaviside function and $u_0(x,y)$ is the given image. To get the minimum of F, we need to take the derivatives of F and set them to 0.

$$c_1(\phi) = \frac{\int_\Omega u_0(x,y) H(\phi(t,x,y)) dxdy}{\int_\Omega H(\phi(t,x,y)) dxdy}, \quad (7)$$

$$c_2(\phi) = \frac{\int_\Omega u_0(x,y)(1-H(\phi(t,x,y))) dxdy}{\int_\Omega (1-H(\phi(t,x,y))) dxdy}, \quad (8)$$

$$\frac{\partial\phi}{\partial t} = \delta(\phi)\left(\nu \text{div}\left(\frac{\nabla\phi}{|\nabla\phi|}\right) - (u_0-c_1)^2 - (u_0-c_2)^2\right), \quad (9)$$

where $\delta(\cdot)$ is the Dirac function.

The active contour model allows to localize the pupillary boundary in spite of a bad estimate of the pupil center. Since the center coordinate of the pupil is estimated by the intensity-based histogram, the initial histogram is not noise-free. Actually the distribution of the histogram is affected by the intensity of the eyelids and eyelashes as well as the highlights at the time the image

is taken. This error of the center coordinates is corrected by the active contour model and a circular Hough transform in our method. Fig. 4 compares two localization results of the pupillary boundary based on an incorrect prior (top row) and on a correct prior (bottom row). Asterisks (*) in the images represent the estimated centers. If the center is initially estimated incorrectly, the segmentation result from the active contour model contains more eyelid regions as in the middle image of the top row in Fig. 4.

At the last step, the inner pupil boundary and the outer pupillary boundary are detected on the basis of the circular Hough transform [14]. The parameters of a circle is modeled as the following circle equation:

$$(x - x_0)^2 + (y - y_0)^2 = r^2, \tag{10}$$

where (x_0, y_0, r) represents a circle to be found with the radius r, and the center coordinates (x_0, y_0). Whether or not the priori center coordinate of the pupil is positioned within the pupil, the segmentation result at least contains the pupillary boundary and the circular Hough transform finds the correct center of the pupil. We expect the model can handle various characteristics of iris patterns in a natural setting.

3.4. Noise Removal

The effect of noises are suppressed twofold. The first attempt is done by region filling where specular highlights generate white holes within the pupil. In addition, the influence of noise are suppressed by a Gaussian blur before finding the edges of the image. The following Gaussian filter, centered at (x_0, y_0) with a standard deviation σ, is used for this purpose.

$$G(x, y) = \frac{1}{2\pi\sigma^2} \exp\left[- \frac{(x - x_0)^2 + (y - y_0)^2}{2\sigma^2} \right], \tag{11}$$

3.5. Iris Segmentation

After localizing the pupil, pixels within the inner circle are marked as background in order to find the outer circle known as the limbic boundary. The circular Hough transform is once again used to estimate the center coordinate and the radius of the circle. Since two boundaries are modeled as circles independently, we apply a rule to two circles that the pupillary boundary circle should be inside the limbic boundary circle. If this condition is not met, an extra round of Hough transform is performed. The final segmentation results are shown in Fig. 5.

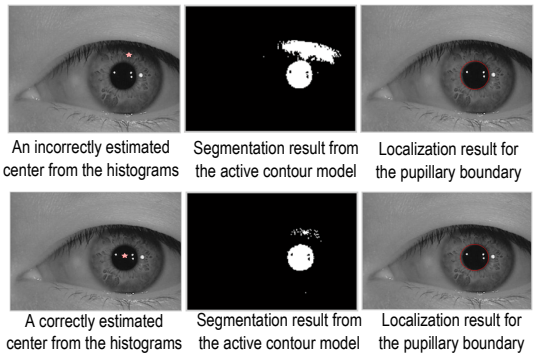

Figure 4. Pupil Localization results based on an incorrect prior (top row) and on a correct prior (bottom row)

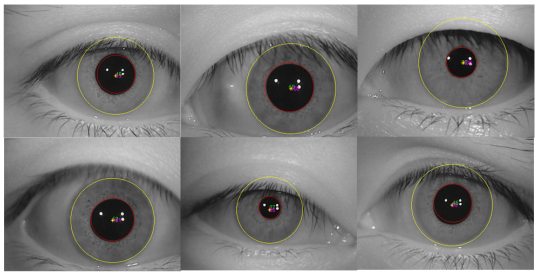

Figure 5. Iris localization results

4. Experiments

4.1. Image Database and Hardware

For the testing of our algorithms we used CASIA iris image database version 3 (The Institute of Automation, Chinese Academy of Sciences) [1]. The CASIA contains a total of 22,035 iris images from more than 700 subjects. For our experiments, images in the *IrisV3-Lamp* subset are used since they contain nonlinear deformations and noisy characteristics such as eyelash occlusion. The experiments were performed in Matlab 7 environment on a PC with Intel Xeon CPU at 2GHz speed and with 3GB physical memory.

4.2. Discussion

The segmentation results are compared against the Daugman's method, known to be the best iris recognition algorithm, as in Table 1. For comparison purpose, Daugman's algorithm is also implemented in Matlab. According to the experimental results on 100 images, the proposed method correctly segment the pupillary and limbic boundaries with 99% accuracy while Daugman's algorithm shows 96% accuracy. Furthermore, it

Method	Accuracy	Mean Elapsed Time
Daugman's Method	96%	569 ms
Proposed Method	99%	232 ms

Table 1. Comparison of performance

runs almost 2.5 times faster. The performance of the iris segmentation is affected by several factors: a threshold for binarization, the number of iterations for the evolving contour, and blurring parameters.

5. Conclusions and Future Work

In this paper, we proposed a robust iris segmentation algorithm that localizes the pupillary boundary and the limbic boundary in the presence of noise. For finding edges of the iris, a region-based active contour model along with a Canny edge detector is used. Noises are reduced by a Gaussian blur and region filling. Experimental results based on 100 images from the public iris image database, CASIA version 3, show that our method achieves an accuracy of 99%. Compared to Daugman's method achieving 96%, it also runs about 2.5 times faster. In the future, we plan to test our algorithm on multiple public iris image databases since CASIA iris database consists mostly of images from Chinese subjects. In addition, segmentation results will be compared against other algorithms.

References

[1] CASIA iris image database. *http://www.cbsr.ia.ac.cn/IrisDatabase.htm*.

[2] T. F. Chan and L. A. Vese. Active contours without edges. *IEEE Transactions on Image Processing*, 10(2):266–277, 2001.

[3] C. Chin, A. Jin, and D. Ling. High security iris verification system based on random secret integration. *Computer Vision and Image Understanding (CVIU)*, 102(2):169–177, 2006.

[4] J. Daugman. High confidence visual recognition of persons by a test of statistical independence. *IEEE Transactions on Pattern Analysis and Machine Intelligence (PAMI)*, 15(11):1148–1161, 1993.

[5] J. Daugman. *Biometrics: Personal Identification in Networked Society*. Kluwer Academic Publishers, 1999.

[6] J. Daugman. Iris recognition. *American Scientist*, 89:326–333, 2001.

[7] J. Daugman. How iris recognition works. *IEEE Transactions on Circuits and Systems for Video Technology (CSVT)*, 14(1):21–30, 2004.

[8] J. Daugman. Probing the uniqueness and randomness of iris codes: Results from 200 billion iris pair comparisons. *Proceedings of the IEEE*, 94:1927–1935, Nov. 2006.

[9] Z. He, T. Tan, and Z. Sun. Iris localization via pulling and pushing. *International Conference on Pattern Recognition '06*, 4:366–369, 2006.

[10] Z. He, T. Tan, Z. Sun, and X. Qiu. Toward accurate and fast iris segmentation for iris biometrics. *IEEE Transactions on Pattern Analysis and Machine Intelligence*, 31(9):1670–1684, September 2009.

[11] L. Ma, T. Tan, Y. W, and D. Zhang. Personal identification based on iris texture analysis. *IEEE Transactions on Pattern Analysis and Machine Intelligence*, 25(12):1519–1533, 2003.

[12] D. Mumford and J. Shah. Optimal approximation by piecewise smooth functions and associated variational problems. *Comm. Pure App. Math.*, 42:577–685, 1989.

[13] L. Pan, M. Xie, and Z. Ma. Iris localization based on multi-resolution analysis. *International Conference on Pattern Recognition '08*, 2008.

[14] M. Sonka, V. Hlavac, and R. Boyle. *Image Processing, Analysis, and Machine Vision*. Thomson Pub., 2008.

[15] R. P. Wildes. Iris recognition: An emerging biometric technology. *Proceedings of the IEEE*, 85(9):1348–1363, 1997.

[16] R. P. Wildes, a. J. C. Asmuth, C. Hsu, R. J. Kolczynski, J. R. Matey, and S. E. McBride. Automated, noninvasive iris recognition system and method. *U.S. Patent*, (5,572,596), 1996.